AD-A116 474 MASSACHUSETTS INST OF TECH CAMBRIDGE DEPT OF ELECTRI--ETC F/G 11/9
IN-SITU MEASUREMENT OF THE PROPERTIES OF CURING SYSTEMS WITH MI--ETC(U)
MAY 82 S D SENTURIA, N F SHEPPARD, H L LEE N00014-78-C-0591
UNCLASSIFIED TR-4 NL

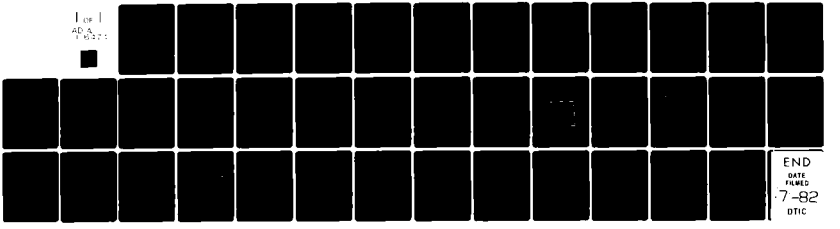

END
DATE FILMED
7-82
DTIC

(12)

OFFICE OF NAVAL RESEARCH

Contract N00014-78-C-0591

Task No. NR 356-691

TECHNICAL REPORT NO. 4

In-situ Measurement of the Properties of Curing Systems with Microdielectrometry

by

S. D. Senturia, N. F. Sheppard, Jr., H. L. Lee,
and David R. Day

~~Paper~~ Presented at
1982 Adhesion Society Meeting
Mobile, ~~Alabama~~
~~February~~, 1982 .

To be Published in Journal of Adhesion

MASSACHUSETTS INSTITUTE OF TECHNOLOGY
Department of Electrical Engineering and Computer Science
and Center for Materials Science and Engineering
Cambridge, Massachusetts

May 4, 1982

UNCLASSIFIED

SECURITY CLASSIFICATION OF THIS PAGE (When Data Entered)

REPORT DOCUMENTATION PAGE	READ INSTRUCTIONS BEFORE COMPLETING FORM
1 REPORT NUMBER	2 GOVT ACCESSION NO. AD-A116 424 / 3 RECIPIENT'S CATALOG NUMBER
4 TITLE (and Subtitle) In-situ Measurement of the Properties of Curing Systems with Microdielectrometry	5 TYPE OF REPORT & PERIOD COVERED Technical Report 6/81-4/82
	6 PERFORMING ORG. REPORT NUMBER Technical Report No. 4
7 AUTHOR(s) S.D. Senturia, N.F. Sheppard,Jr., H.L. Lee, and D.R. Day	8 CONTRACT OR GRANT NUMBER(s) N00014-78-C-0591
9 PERFORMING ORGANIZATION NAME AND ADDRESS Massachusetts Institute of Technology Department of Electrical Engineering and Computer Science, Cambridge MA 02139	10 PROGRAM ELEMENT, PROJECT, TASK AREA & WORK UNIT NUMBERS NR 356-691
11 CONTROLLING OFFICE NAME AND ADDRESS Department of the Navy, Office of Naval Research 800 N. Quincy Street, Arlington VA 22217 Code 427	12 REPORT DATE 4 May 1982
	13 NUMBER OF PAGES 32
14 MONITORING AGENCY NAME & ADDRESS(if different from Controlling Office)	15 SECURITY CLASS. (of this report) UNCLASSIFIED
	15a DECLASSIFICATION/DOWNGRADING SCHEDULE

16 DISTRIBUTION STATEMENT (of this Report)

This document has been approved for public release and sale; its distribution is unlimited.

17 DISTRIBUTION STATEMENT (of the abstract entered in Block 20, if different from Report)

18 SUPPLEMENTARY NOTES

19 KEY WORDS (Continue on reverse side if necessary and identify by block number)

Dielectrometry, cure monitoring, epoxy, integrated circuit, diglycidyl ether of bisphenol-A, metaphenaminediamine, phenyl glycidyl ether, diaminodiphenyl-sulfone, microdielectrometry, diluent

20 ABSTRACT (Continue on reverse side if necessary and identify by block number)

This paper reports the measurement of low frequency dielectric properties of several epoxy-amine systems undergoing cure. Results from isothermal cures of DGEBA-MPDA are shown to provide a measurement of a low-frequency relaxation time that can be correlated with bulk viscosity prior to gelation. Also studied was the effect of PGE diluent in the DGEBA-DDS system. It is shown that as little as 5 phr diluent produces observable changes in the low-frequency dielectric properties.

DD FORM 1 JAN 73 1473 EDITION OF 1 NOV 65 IS OBSOLETE S/N 0102-LF-014-6601

UNCLASSIFIED

SECURITY CLASSIFICATION OF THIS PAGE (When Data Entered)

IN-SITU MEASUREMENT OF THE PROPERTIES OF CURING SYSTEMS WITH MICRODIELECTROMETRY

S. D. Senturia, N. F. Sheppard, Jr., H. L. Lee, and D. R. Day

Massachusetts Institute of Technology

I. INTRODUCTION

As new materials and cure methods are developed, the ability to make direct measurements of the properties of curing systems is central both to the analysis of the effects of a modified material or cure method, and to the evaluation of the resulting materials for practical applications. Mechanical and rheological methods address macroscopic properties, while spectroscopic methods address properties on a microscopic molecular level. Dielectric methods share both macroscopic and microscopic features, in that the dipoles being oriented during dielectric measurements are of microscopic origin, whereas the degree and speed of their orientation may depend on macroscopic properties of the curing system, such as viscosity and the tightness of the cross-linked network.

This paper addresses the in-situ measurement of various properties of curing systems with a particular dielectric method called Microdielectrometry (1,2,3). We have used integrated circuit technology to develop a miniaturized dielectric probe that combines small size with built-in amplification to achieve sensitivity at frequencies as low as 1 Hz. The device combines a planar interdigitated electrode structure with a pair of matched field-effect transistors. Calibration is based entirely on the

details of the electrode geometry, and thus is stable with respect to temperature variations, and is reproducible from device to device. The Microdielectrometer "chip" can be implanted in a bulk specimen, or it can be used by placing a few milligrams of sample on the active device region. With suitable packaging, the device can be used in a wide range of environments, and can function at temperatures up to 250 C.

We have used Microdielectrometry to follow the changing low frequency dielectric properties of a variety of curing systems, including amine cured epoxies, polyimides, phenolics, and various rubbers. Generally, what we measure is the frequency dependent dielectric permittivity (ε') and dielectric loss factor (ε'') in the frequency range 1-1000 Hz. In the specific cases to be discussed in this paper, these dielectric properties are interpreted in terms of more fundamental properties of the system, such as viscosity, and the structure of the cross-linked network.

We have studied isothermal cures of diglycidyl ether of bisphenol A (DGEBA) with m-phenylene diamine (MPDA) at temperatures in the range 60-100 C. The variation of ε' and ε'' with frequency at any instant of cure prior to gelation can be used to determine a low-frequency dielectric relaxation time, τ, which can be correlated with the bulk viscosity. We have also examined the effect of the diluent phenyl glycidyl ether (PGE) on DGEBA cured with diaminodiphenylsulfone (DDS), both during cure at 140 C and in post-cure ramped temperature studies. It is found that as little as 5% diluent produces observable changes in the low-frequency dielectric properties, and that frequencies below 10 Hz are more sensitive than higher frequencies to the effects of the dominant low-frequency dielectric relaxation associated with the glass transition.

II. EXPERIMENTAL

A. Microdielectrometry.

The usual method for making measurements of dielectric properties is to place the sample between closely spaced parallel conducting plates, and to monitor the AC equivalent capacitance and dissipation factor of the resulting capacitor. The capacitance is proportional to the dielectric permittivity (ε') at the measurement frequency, and the dissipation factor in combination with the ε' value can be used to extract the dielectric loss factor (ε''). The calibration of the measurement depends on the area of the plates and on their spacing. When used for in-situ measurements in curing systems, plate spacing can change with either temperature or stress, with the result that the calibration for ε' and ε'' can be affected. However, since both calibrations are affected equally by geometry changes, their ratio, the loss tangent ($= \varepsilon'/\varepsilon''$), is not affected. Hence, when making conventional measurements, one often monitors loss tangent rather then ε' or ε'' during cure.

The approach taken in Microdielectrometry is fundamentally different. Instead of using a parallel plate geometry, both electrodes used in the dielectric measurement are placed on the same surface of an integrated circuit (see Fig. 1 for a schematic top view), and the medium to be studied is placed over the electrodes, either by application of a small sample or by embedding the entire integrated circuit in the curing medium (see Fig. 2 for a schematic cross section through the electrode region). Because this electrode geometry is less efficient than parallel plates in terms of coupling the electric field through the sample medium, amplification is required in the form of a field-effect transistor whose gate electrode is one

of the two interdigitated electodes (called the floating gate; see Fig. 1). To compensate for the transistor amplification factor, which would require a complex calibration procedure at each operating temperature, a second identical field-effect transistor is simultaneously fabricated on the same integrated circuit (see Fig. 3 for a microphotograph of the device). The second field-effect transistor serves as a reference in a differential feedback circuit, the details of which have been published elsewhere (4). The net effect of the two-transistor plus feedback circuit combination is that when a sinusoidal signal is applied to the driven electrode, the corresponding sinusoidally varying voltage that appears on the floating gate can be measured independent of transistor amplification factor. This floating-gate voltage has an amplitude and phase relative to the drive signal that depends on the geometry of the device and on the dielectric properties of the sample medium. The device geometry is both stable and reproducible. Thus, the task of calibrating the measurement reduces to relating the measured amplitude and phase for a particular device geometry to the specific values of ε' and ε'' for the sample.

We have developed a computerized instrumentation system for use in Microdielectometry (see Fig. 4). A Hewlett-Packard HP85 calculator serves as controller and data-logger. Archival data storage is done on tape cassettes. Provision is made for making programmed measurements at many different frequencies, and for monitoring temperature during the experiment. The calibration of the basic amplitude-phase data in terms of ε' and ε'' (see below) is stored in the caculator memory as a lookup table that is used in conjunction with an interpolation program. The system also has provision for

operating a line printer and a graphics plotter, and data files can be transferred to other computers such as our laboratory's HP-1000 if large-scale computations are required.

B. Calibration.

The fact that the sensing electrode is electrically floating, combined with the proximity of the amplifier to that electrode, means that good signal-to-noise ratio can be achieved at very low frequencies. However, the electrode geometry is more difficult to calibrate than conventional parallel plates. We have approached the calibration problem by setting up a computer solution to the two-dimensional Laplace equation for our device geometry assuming that the material is both isotropic and homogeneous (5). This approach ignores surface and electrode effects, but permits a calculated calibration to be obtained for all ranges of ε' and ε''. Figure 5 shows a typical set of calibration curves. Each measurement yields an amplitude (gain in decibels) and a phase (in degrees). Contours of constant ε' and ε'' are plotted in this gain-phase space, permitting the interpretation of measured data in terms of dielectric properties.

Experimental verification (and/or modification) of the calculated calibration is made difficult by the intrinsic problem of preparing calibration materials with known dielectric permittivity and loss factor. Along the gain axis, however, which corresponds to low loss factor, the contours of constant ε'' bunch together. Therefore, for low-loss materials, there is a direct correspondence between ε' and gain. We have verified the calculated ε' values along this axis with various low-loss dielectric fluids and with the bare device in air ($\varepsilon' = 1.0$), and find agreement to better than

10%. However, at low values of ε'', any errors in phase measurement will limit the precision of the ε'' determination. For our present device design, packaging, cabling arrangement, and choice of phase-measurement instrument (HP 3575A), phase measurements corresponding to ε'' values below about 0.02 cannot be reliably interpreted. There is nothing fundamental about this limitation; it represents the present state of our progress with the calibration.

There is another difficult portion of the gain-phase space, corresponding to high loss factors, where the contours of constant ε' bunch together. In this region, accurate determination of ε' is difficult. Furthermore, any small measurement errors, either in gain or phase, can produce errors in both ε' and ε'' in this high-loss region. Our present capabilities allow measurement of ε'' up to about 100, and measurement of ε' wherever ε'' is less than about 30. Outside these limits, the calibration is not valid at present.

In the central region of the gain-phase space, where contours are well spaced, there is adequate sensitivity to determine both ε' and ε'' to within a few percent. However, the absolute accuracy of the calibration in this region has not yet been established. Comparison measurements made on nominally identical samples using devices with different geometries are being done to explore this issue.

C. Samples and Measurements.

The materials used in this study were a bifunctional epoxy, diglycidyl ether of bisphenol A (DGEBA), having an epoxide equivalent weight of 175; a

reactive epoxide diluent, phenyl glycidyl ether (PGE); and two amine curing agents, m-phenylene diamine (MPDA), and diaminodiphenyl sulfone (DDS). All epoxy-amine samples were prepared in 2-3 gram batches using a stoichiometric amount of epoxide and amine functionalities. The components were weighed out, melted together over low heat until dissolved, cooled, and stored in a refrigerator until use, for at most a period of a week.

Microdielectrometer chips having aluminum electrodes with a between electrode spacing of 12 microns and having electrode-to-substrate spacings of both 1000 nm and 540 nm were fabricated using standard MOS technology in the MIT Microelectronics Laboratory (4). The individual chips were attached to TO-99 transistor headers, and leads were attached using ultrasonically bonded 1 mil aluminum wire. The resin samples were applied to the electrode area by first heating the resin slightly until it flowed, then applying a few drops with an eyedropper. The experiments were performed in the oven of a modified gas chromatograph, which permitted isothermal or programmed ramp temperature cycles.

III. RESULTS

A. DGEBA-MPDA.

Typical results (6) for the time dependence of ε' and ε'' for the DGEBA-MPDA system at 60 and 100 C are shown in Figs. 6 and 7. Data are presented for three frequencies (a total of seven were measured), and for devices with electrode-to-substrate spacing of 1000 nm (devices with 540 nm spacing were also used). Times to gelation t_g for this resin system are also shown for reference (7). Comparison between Figs. 6 and 7 shows that the

behavior of the dielectric properties is similar, but occurs over a longer time scale as the temperature is decreased.

An obvious result from the data is that both ε' and ε'' are strongly dispersive (i.e., frequency dependent). Hindered dipole rotation and hindered bulk conduction (presumed ionic) can each lead to such dispersion. The ideal Debye model for hindered rotation is illustrated in Fig. 8. When the product $\omega\tau$ is small (ω is the angular frequency, τ the dielectric relaxation time), the permittivity is large, and the loss is low. Near $\omega\tau = 1$, ε' decreases and ε'' has a peak. For large $\omega\tau$, the permittivity is low and the loss is low. The effect of a constant bulk conductivity is to add a term to ε'' equal to the conductivity divided by the frequency. However, if the conductivity mechanism is itself a hindered process, with its own relaxation time, such a conductivity gives rise both to a modified ε'' and to a term in ε' which has the same form as for the Debye model. In the discussion to follow, we shall concentrate on the apparent Debye-like behavior of ε' and ε'' observed in this particular system, while for the experiments reported in the following section, we shall note the added presence of an apparent bulk conductivity contribution to ε'' early in cure. In neither case can we prove whether the observed Debye-like behavior is due to the hindered dipole rotation or to the hindered conduction mechanism, particularly for the pre-gelation behavior where the conductivity might be expected to be large.

Turning now to the data, and with the Debye model in mind, one can see that Figs. 6 and 7 show two Debye-like relaxations: a large relaxation prior to gelation, and a smaller relaxation after gelation. The frequency dependence demonstrates that the 1 Hz measurement is more sensitive to these relaxations than higher frequencies. Increased frequency or increased extent of cure make it more difficult for the dipoles to respond to the alternating electric field.

The pre-gelation data from all six experiments (three temperatures, two

device geometries) were fitted to the ideal Debye model, and the time- and temperature-dependent dielectric relaxation time was extracted, as shown in Fig. 9. For any one device, the agreement between the relaxation times determined from different frequencies at the same elapsed cure time was within 20%, whereas the agreement between the relaxation times determined from the devices with different oxide thicknesses at the same cure temperature was within 50%. Since the relaxation time changes by many orders of magnitude during cure, this degree of agreement is already very good. However, the results indicate that further refinements of the calibration may be required.

The time dependence of the pre-gelation relaxation time resembles the time dependence of the viscosity of thermosetting systems. For example, the slope of a log viscosity versus time plot breaks to a much steeper value as cure proceeds, which is attributed to chain entanglement among the branched polymers formed early in cure (8). In addition, at the start of cure, the higher temperature sample has a lower viscosity, but cures faster, so its viscosity versus time curve will cross the corresponding curve for a lower temperature. The data of Fig. 9 show both these features. To illustrate the excellent correspondence between our relaxation-time data and the viscosity data reported by Kamal (9), Fig. 10 shows an Arrhenius plot of the time to reach 8 sec relaxation time and Kamal's time to reach 400 poise viscosity. The points fall on a single line characterized by an activation energy of 11.5 Kcal/mole, indicating that the same process is responsible for the behavior of both the viscosity and the pre-gelation relaxation time.

B. PGE Diluent in DGEBA-DDS.

Phenyl glycidyl ether (PGE) is a monofunctional epoxide which can react with an amine functionality, reducing the ability of the system to form crosslinks. We have examined the effects of various amounts of PGE in DGEBA

cured with diaminodiphenyl sulfone (DDS). DDS is tetrafunctional, but the the effect of adding PGE diluent can be viewed as reducing the effective functionality of the amine. At 33 phr, the effective amine functionality becomes 3, and at 100 phr, the functionality becomes 2, at which point the system tends to form linear polymer rather than a crosslinked continuous network.

Figures 11 and 12 show ε' and ε'', respectively, versus cure time at 140°C for each of four frequencies (1, 10, 100 and 1000 Hz) for various amounts of diluent. Measurements were also made at 100 phr, with results almost identical to the 80 phr data. The data in the Figures at high loss factor have been manually smoothed to improve visibility. The raw data showed considerable noise above ε' values of 30, consistent with the calibration difficulties described earlier.

Referring first to Fig. 11, the post-gelation relaxation, at least for 0, 20, and 40 phr resembles the results presented for the DGEBA-MPDA system. The pre-gelation relaxation observed for the DGEBA-MPDA system (Fig. 6 and 7), and expected at 90 min. for this system based on the data of Babayevsky and Gillham (10), is not seen in Fig. 11 because the relatively high bulk conductivities which occur at low cure times result in data that are beyond the present calibration capability. (The effect of a bulk conductivity is to add to ε'' a term equal to the conductivity divided by the frequency.) The conductivity decreases with cure time, but is still large enough to wash out the post-gelation loss peaks in Fig. 12, except at 1000 Hz.

The most striking feature of the data is the similarity of the general shapes of the data for all diluent levels, excepting only the marked slowing of the apparent cure rate with increasing amounts of diluent. In the case of 80 phr, the data show that the cure reaction has almost ceased at 360 min. yet the ε' values at low frequencies have not decreased nearly as much as

those ε' values of less diluted samples for corresponding times. This is consistent with the presence of diluent. That is, with diluent present, fewer crosslinks are formed, and the reaction ceases with a molecular network that is similar to what a partially cured non-diluted sample would exhibit if quenched during cure. This suggests that the glass transition temperatures of the samples should show a steady decrease with increasing amounts of diluent, and a post-cure ramped temperature experiment was carried out to examine this possibility.

Figures 13 and 14 show the ε' and ε'' data at 1 Hz for a set of samples first cured at 140 °C for six hours, then cooled to room temperature, then subjected to a temperature ramp at 1 deg/min up to 150 C. Referring first to Fig. 13, note the clear 1 Hz dielectric relaxation between 90 and 120 C for the 40 phr sample. This relaxation goes between ε' values of 5 and 14, and corresponds to what would be expected for the glass transition. Note also that at 80 phr, the corresponding relaxation is completed by 85 C, while for 20 phr, it is just beginning at 125 C. For the undiluted specimen, only the faintest onset of this relaxation is evident, even at 150 C, which is 10 degrees above the cure temperature.

The ε'' post-cure data of Fig. 14 correspond to what would be expected from the ε' data, provided a thermally activated conductivity term is added to ε''. The initial increase in ε'' with temperature (Fig. 14) result from dipole relaxations and agrees with what would be expected from the corresponding ε' relaxations (Fig 13). After the plateau in ε'' (the peak of the dipole loss) the thermally activated conductivity takes over causing a continued increase in ε'' with temperature. For the undiluted specimen, only slight evidence of the dipole relaxation is evident at 150 C.

The large sensitivity of the post-cure ε'' data to diluent concentration led us to perform additional experiments with 5 and 10 phr. The ε'' data for post-cure temperature ramps are shown in Fig. 15. Note that as little as 5 phr diluent produces observable changes in the ε'' value at 1 Hz. Note further that even with 10 phr diluent, the 1 Hz dielectric relaxation peak associated with the glass transition has not yet appeared, even at 150 C for samples cured six hours at 140 C.

All of the post-cure data can be summarized by somewhat arbitrarily selecting the "1 Hz loss peak temperature" as indicative of the glass transition. Using the Debye model for interpretation of the ε' data, this temperature corresponds to the point at which $\varepsilon' = 10$. The $\varepsilon' = 10$ temperature is plotted against diluent concentration in Fig. 16. If this were a true plot of glass transition, one would expect the zero diluent case to have a point at 140 C, the cure temperature, and the diluted samples to have progressively lower glass transition temperatures (11). In our case, even the 20 phr sample has not gone through its loss peak at 140 C. However, the general behavior of the data with diluent concentration is reasonable. The conclusion from these results is that in spite of the fact that 1 Hz is a very low frequency at which to make dielectric measurements, it is still not low enough to be considered "near zero". If one raises the undiluted specimen to the temperature at which it was cured, internal dipole orientations at 1 Hz are still effectively quenched. One must raise the temperature well above 140 C before a 1 Hz measurement will show a loss peak. In our case, even with 20 phr, the loss peak at 1 Hz occurs above the cure temperture.

IV. DISCUSSION

This paper has demonstrated the use of Microdielectrometry for the study of curing in two epoxy-amine systems. A major conclusion is that for studies of the networks formed during cure, there is a significant advantage in being able to extend the low-frequency limit of the experiment as far as possible. Indeed, with the diluent example, it is seen that even 1 Hz, which is already well below the lowest frequency available with conventional dielectric instrumentation, is still "too high" to make accurate glass transition temperature determinations. Furthermore, our results clearly demonstrate the value of being able to make measurements at multiple frequencies in real time. For example, the frequency dependence of ε' and ε'' at any instant can be analyzed in terms of models of dielectric relaxation, such as the viscosity in the case of pre-gelation data.

An important direction for future work, in addition to further exploration of the dielectric properties of networks formed with diulent, is to extend the measurement technique to even lower frequencies. Work is presently under way on a Fourier transform spectroscopy equivalent of Microdielectrometry, with which the low frequency limit should be easily extendable to 0.1 Hz or below.

ACKNOWLEDGEMENTS

This work was sponsored in part by the Office of Naval Research. The authors wish to thank Dr. L.H. Peebles, Jr., of ONR for his encouragement and for his welcome participation in technical discussions related to this program. Devices used in this work were fabricated in the M.I.T. Microelectronics Laboratory, a Central Facility of the Center for Materials Science and Engineering, which is sponsored in part by the National Science Foundation under Contract DMR-78-24185. Resins and curing agents used in these experiments were provided by Dr. N. Schneider of the Army Materials and Mechanics Research Center, Watertown, MA. Some of the equipment in the Microdielectrometry apparatus was purchased under NSF Contract ENG-7717219.

REFERENCES

1. N. F. Sheppard, Jr., S. L. Garverick, D.R. Day, and S. D. Senturia, Microdielectrometry: A New Method for In-Situ Cure Monitoring, Proc. 26th SAMPE Symposium, Los Angeles, CA, 26, 65-76 (1981).
2. S. D. Senturia, N. F. Sheppard, Jr., S. L. Garverick, H. L. Lee, and D. R. Day, "Microdielectrometry", Proc. A Critical Review: Techniques for the Characterization of Composite Materials, Cambridge MA, June 1981, in press.
3. N. F. Sheppard, Jr., D. R. Day, H. L. Lee, and S. D. Senturia, "Microdielectrometry", Proc. Materials Research Soc., Boston MA, Nov. 1981, Sensors and Actuators, in press.
4. S. L. Garverick and S. D. Senturia, "An MOS Device for AC Measurement of Surface Impedance with Application to Moisture Monitoring", IEEE Trans. Elec. Dev., ED-29, 90-94 (1982).
5. H. L. Lee, S. M. Thesis, Massachusetts Institute of Technology, 1982, unpublished.
6. The results reported here have been previously published in Refs. 2 and 3. They are included here to illustrate the relaxation time approach to intepreting such data.
7. S. Sourer and M. R. Kamal, "Differential Scanning Calorimetry of Epoxy Cure: Isothermal Cure Kinetics", Thermochimica Acta, 14, 41 (1976).
8. F. G. Musatti and C. W. Macosko, "Rheology of Network Forming Systems", Polymer Eng. Sci., 13 , 236 (1973).
9. M. R. Kamal, S. Sourer, and M. Ryan, "Integrated Thermo-Rheological Analysis of the Cure of Thermosets", Soc. Plast. Eng. 31st Annual Tech. Conf., Montreal, May 1973, p. 187.

10. P. G. Babayevsky and J. K. Gillham, "Epoxy Thermosetting Systems: Dynamical Mechanical Analysis of the Reactions of Aromatic Diamines with Diglycidyl Ether of Bisphenol A", J. Appl. Polymer Sci., 17, 2067-2088 (1973).

11. J. K. Gillham, "Formation and Properties of Network Polymeric Materials", Polymer. Eng. Sci., 19, 676 (1979).

FIGURE CAPTIONS

Fig. 1. Schematic view of active portion of Microdielectrometer chip. CFT refers to "floating-gate charge low transistor", of which the Microdielectrometer is an example.

Fig. 2. Schematic cross-section through electrode region.

Fig. 3. Photomicrograph of chip. Dimensions are 75 x 75 mils.

Fig. 4. Block diagram of Microdielectrometry instrumentation.

Fig. 5. Calculated calibration curves for the Microdielectrometer chip.

Fig. 6. Time dependence of ε' and ε'' for DGEBA-MPDA cured at 60°C.

Fig. 7. Time dependence of ε' and ε'' for DGEBA-MPDA cured at 100°C.

Fig. 8. Dependence of ε' and ε'' on the $\omega\tau$ product for an ideal Debye relaxation.

Fig. 9. Time- and temperature-dependence of the dielectric relaxation time of DGEBA-MPDA prior to gelation.

Fig. 10. Arrhenius plot showing correlation between dielectric relaxation time and viscosity (Ref. 9).

Fig. 11. Permittivity ε' versus cure time at 1, 10, 100, and 1000 Hz for 0, 20, 40, and 80 phr PGE in DGEBA-DDS. Cure is at 140°C.

Fig. 12. Loss factor ε'' corresponding to the conditions of Fig. 11.

Fig. 13. Post-cure behavior of ε' behavior at 1 Hz for DGEBA-DDS diluted with PGE. Heating rate is 1°/min.

Fig. 14. Loss factor data corresponding to Fig. 13.

Fig. 15. Loss factor data at 0, 5, 10, and 20 phr PGE in DGEBA-DDS measured at 1 Hz. Heating reat is 1°/min.

Fig. 16. Effect of PGE concentration on 1 Hz relaxation temperature.

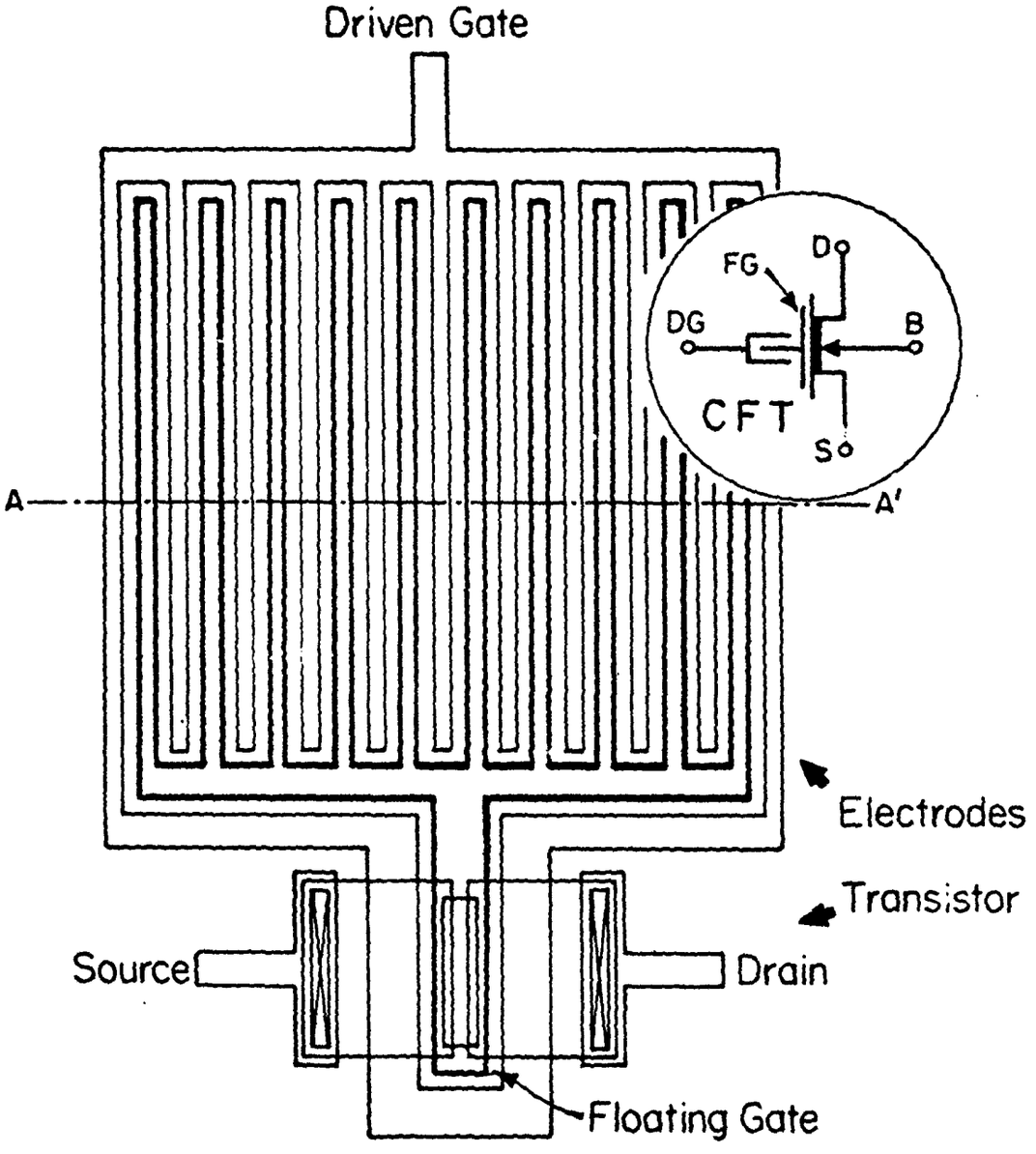
Driven Gate
FG
D
DG
B
CFT
S
A
A'
Electrodes
Transistor
Source
Drain
Floating Gate

Fig. 1

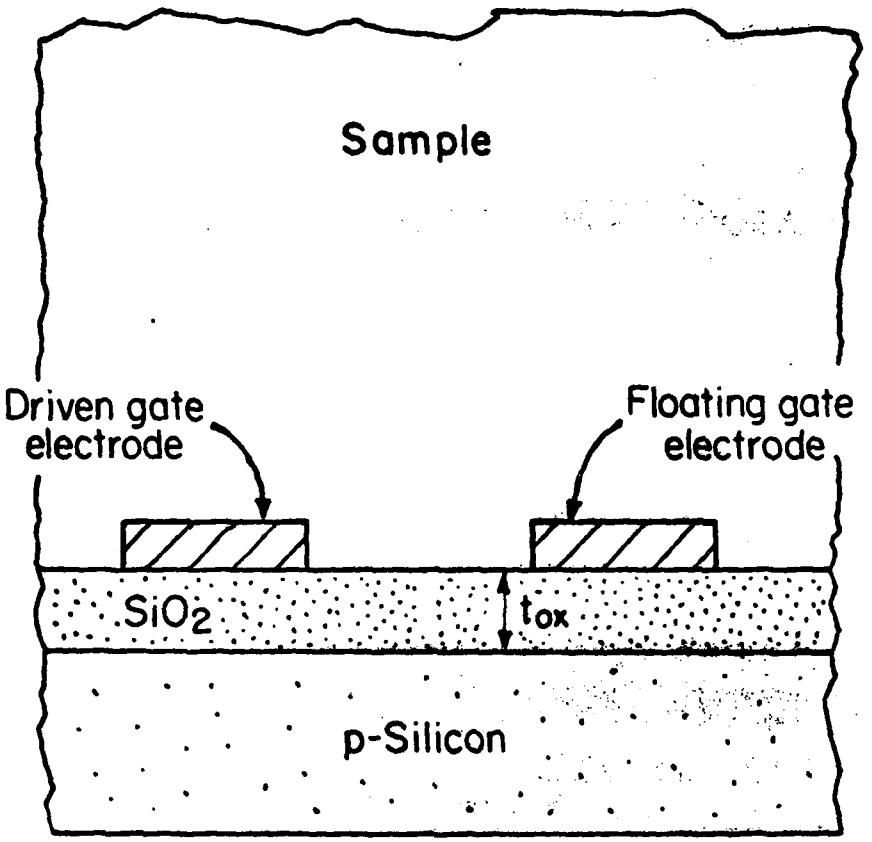
Sample
Driven gate electrode
Floating gate electrode
SiO_2
t_{ox}
p-Silicon

FIG. 2

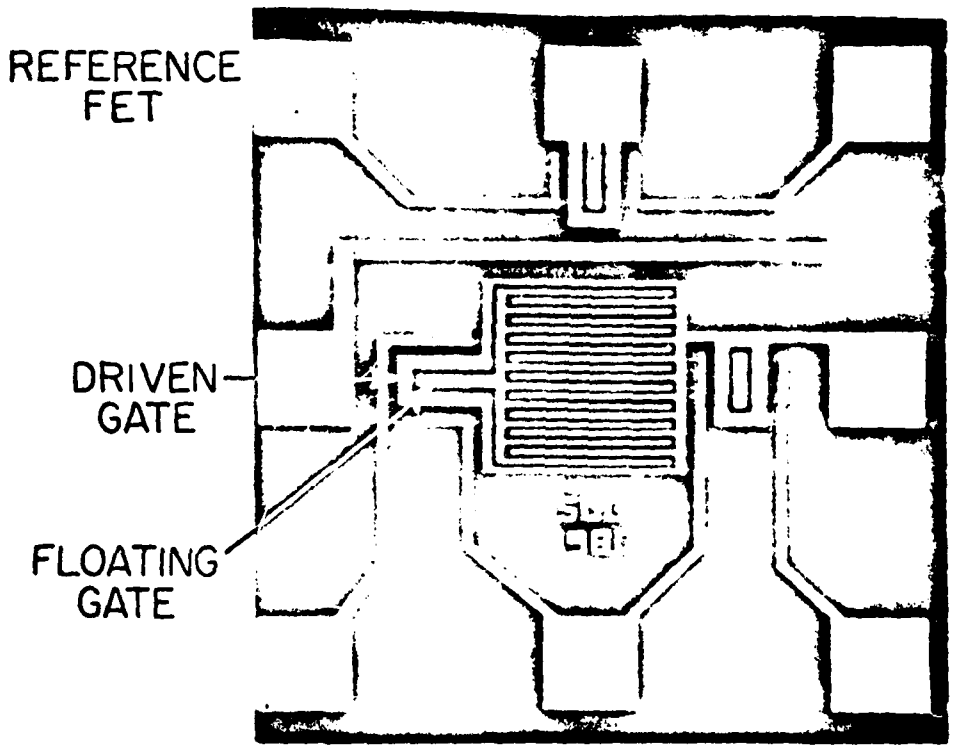

FIG. 3

MEASUREMENT SYSTEM

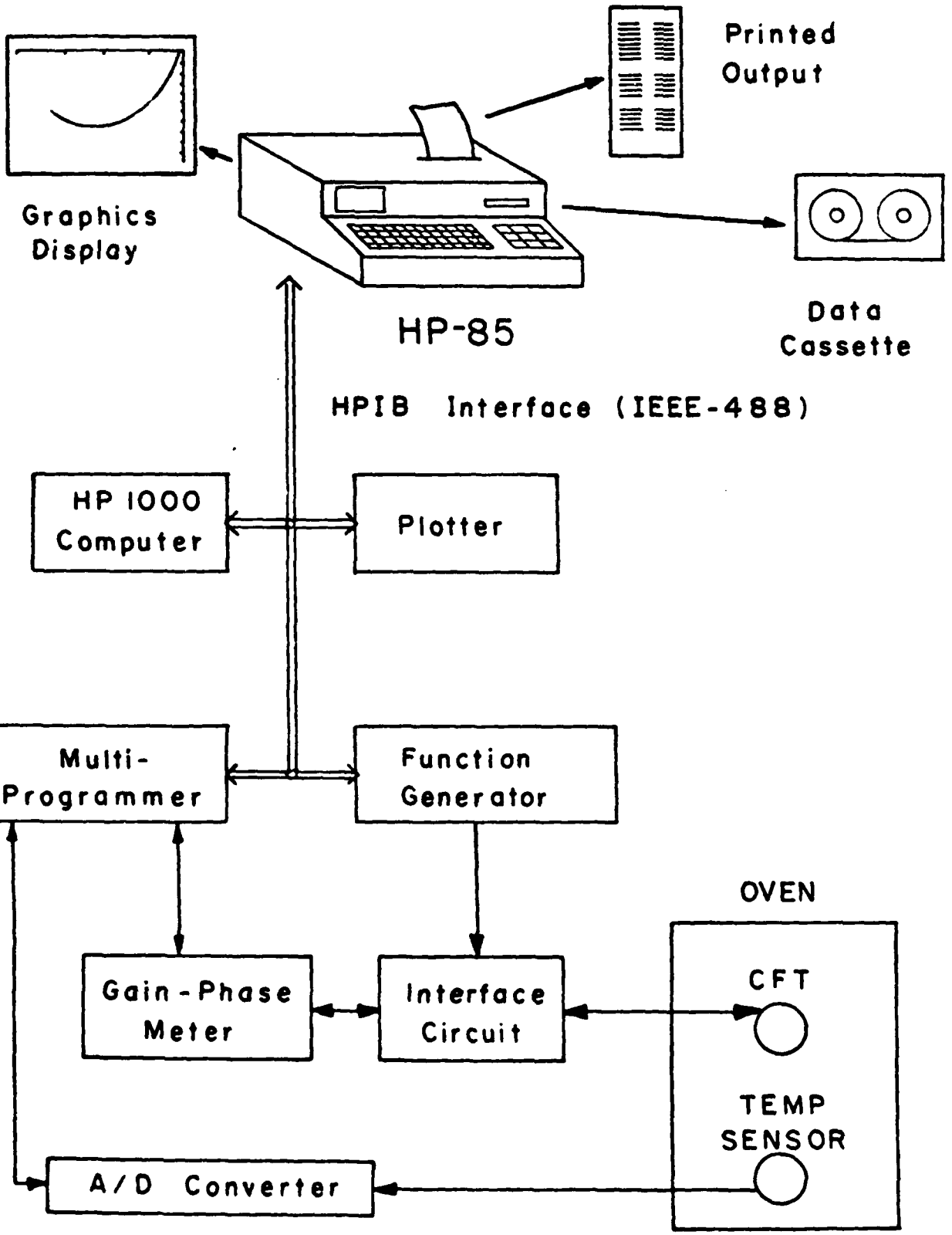

FIG. 4

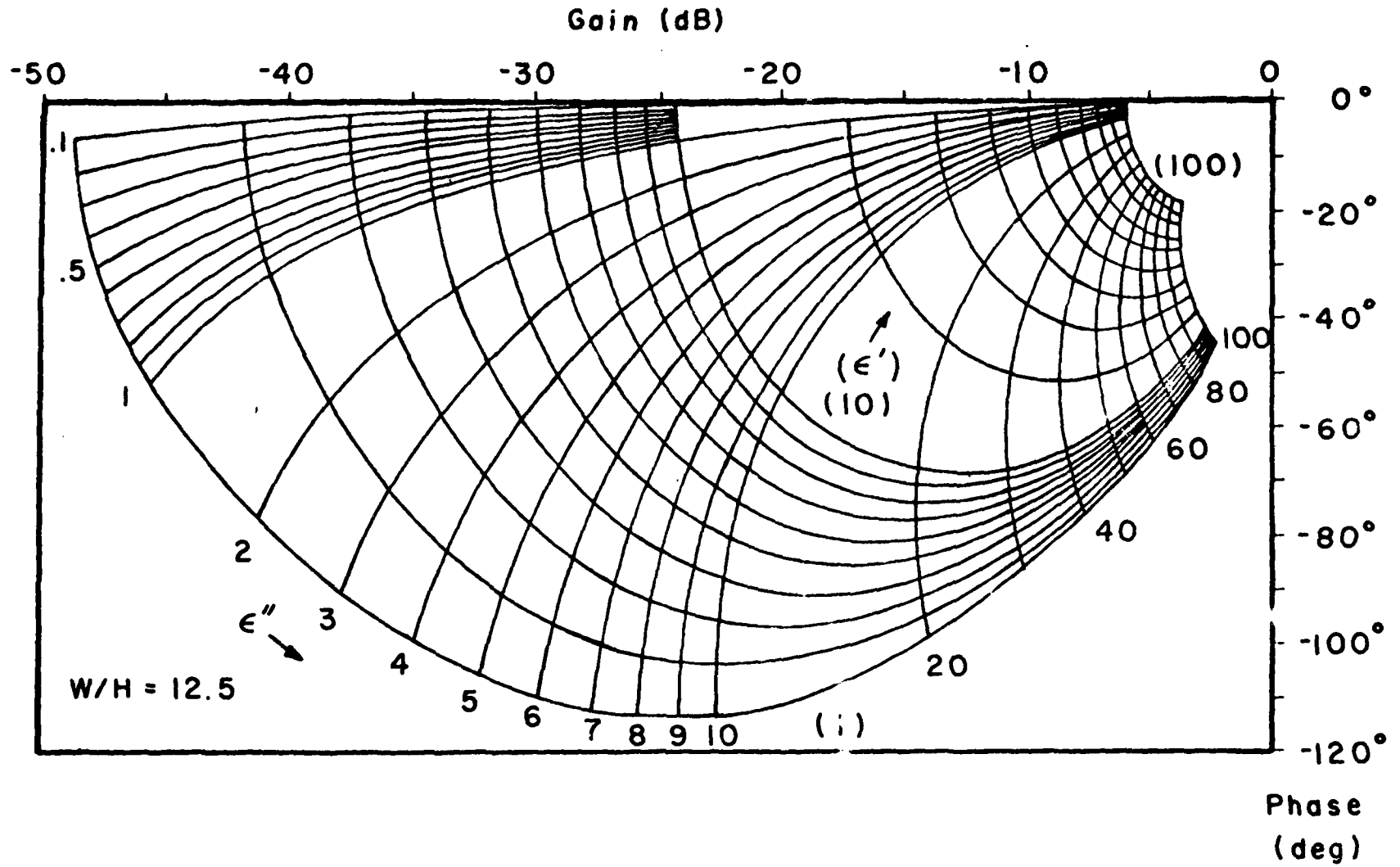
Gain (dB)
-50
-40
-30
-20
-10
0
0°
-20°
-40°
-60°
-80°
-100°
-120°
Phase
(deg)
.1
.5
1
2
3
4
5
6
7
8
9
10
(∞)
20
40
60
80
100
(100)
(ε')
(10)
ε"
W/H = 12.5

FIG. 5

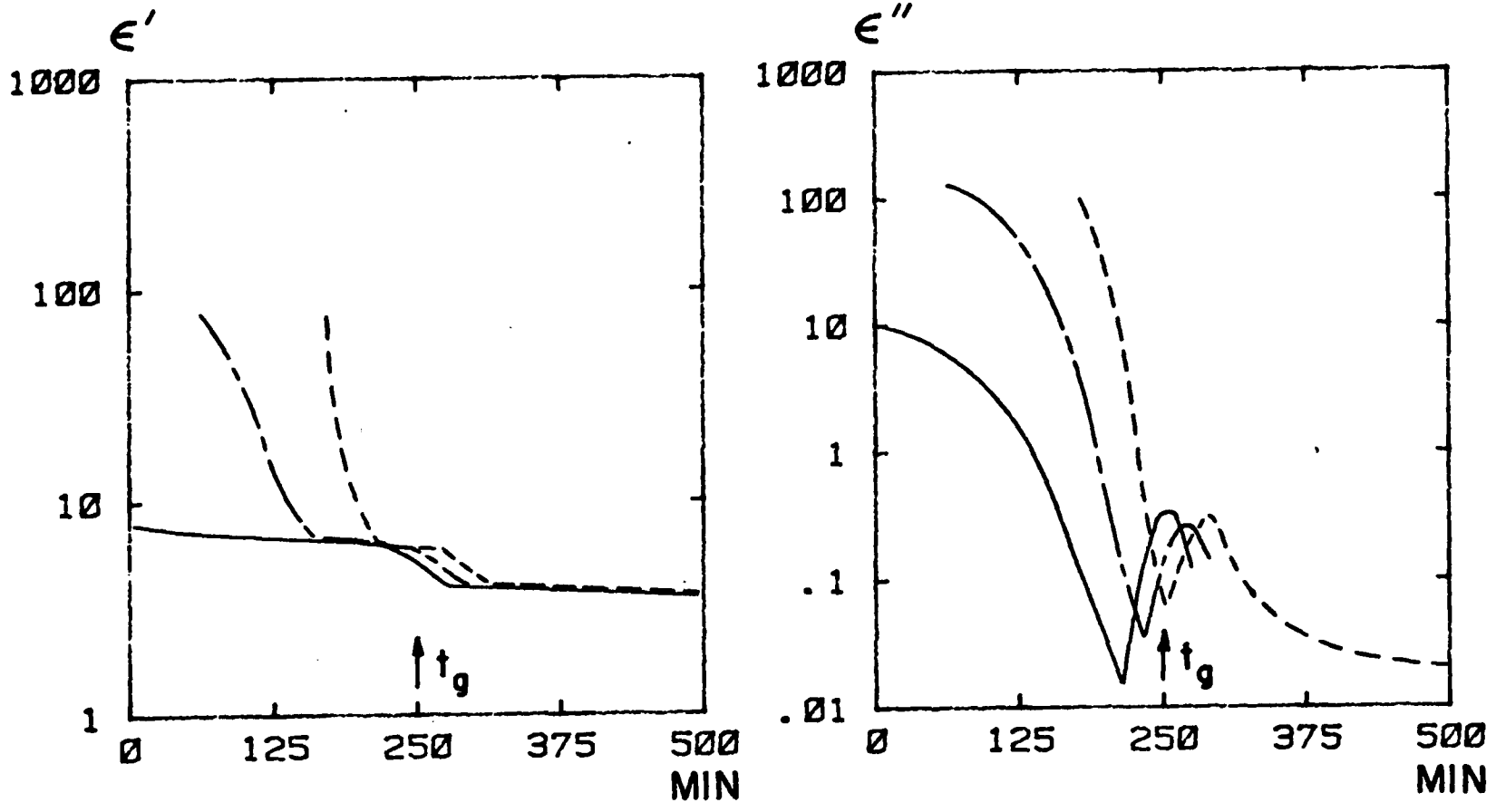
ε′
1000
100
10
1
0
125
250
375
500
MIN
t_g
ε″
1000
100
10
1
.1
.01
0
125
250
375
500
MIN
t_g
1 Hz
30 Hz
1000 Hz
T = 60°C
t_{ox} = 10000 Å

F-16

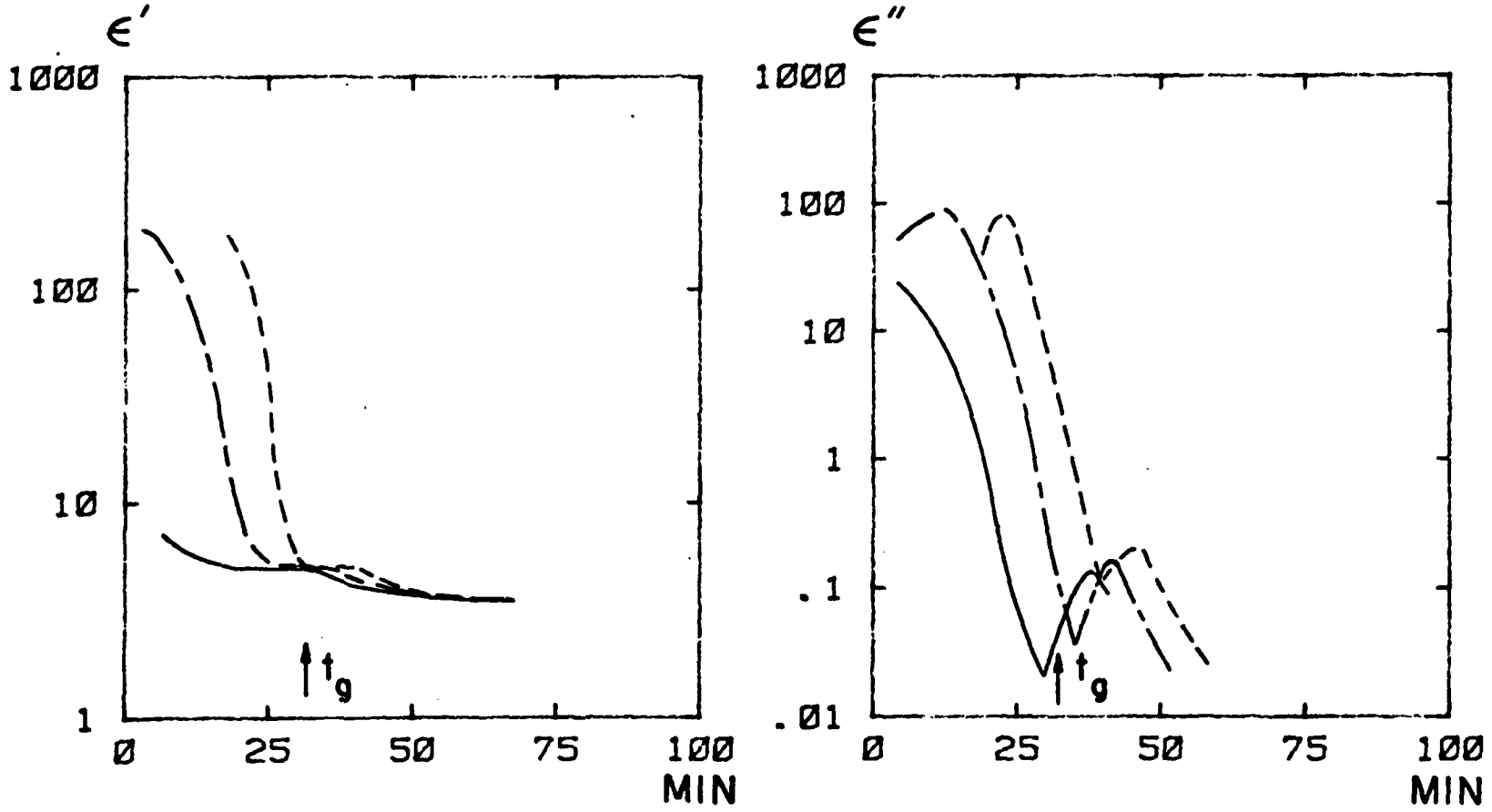
ε′
1000
100
10
1
0
25
50
75
100
MIN
t_g
ε″
1000
100
10
1
.1
.01
0
25
50
75
100
MIN
t_g
1 Hz
30 Hz
1000 Hz
T = 100 °C
t_{ox} = 10000 Å

Fig. 7

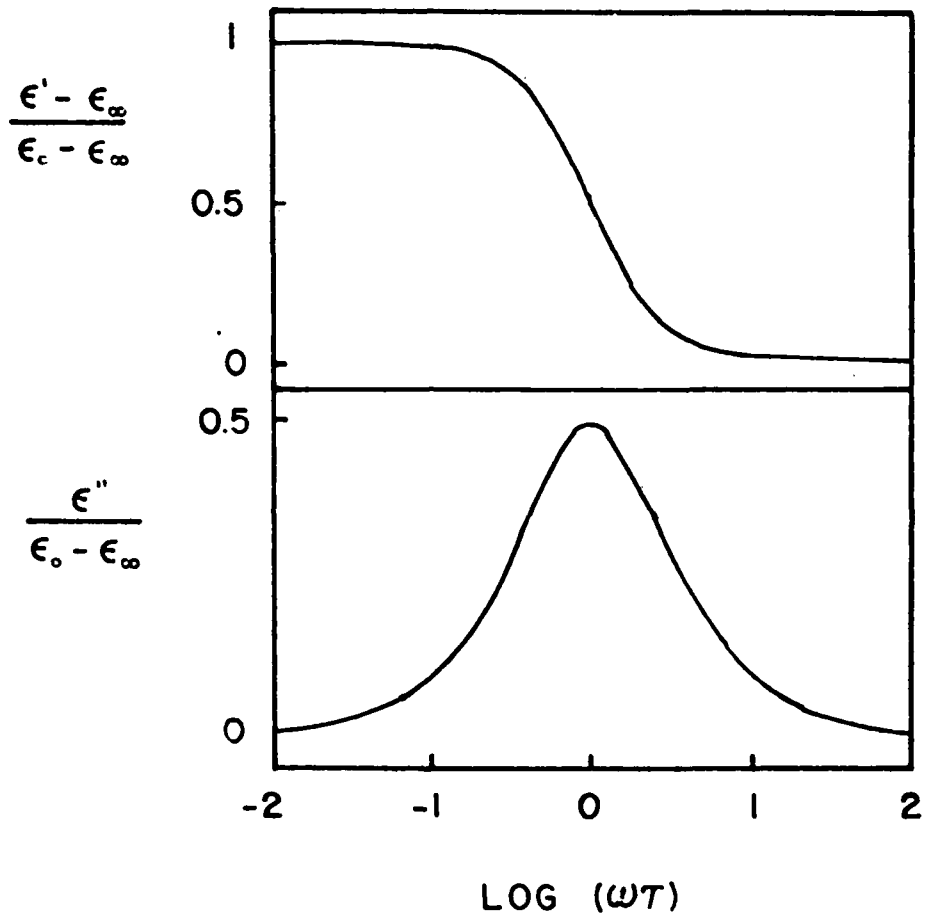
$\frac{\epsilon' - \epsilon_\infty}{\epsilon_c - \epsilon_\infty}$
1
0.5
0
$\frac{\epsilon''}{\epsilon_o - \epsilon_\infty}$
0.5
0
-2
-1
0
1
2
LOG (ωT)

FIG. 8

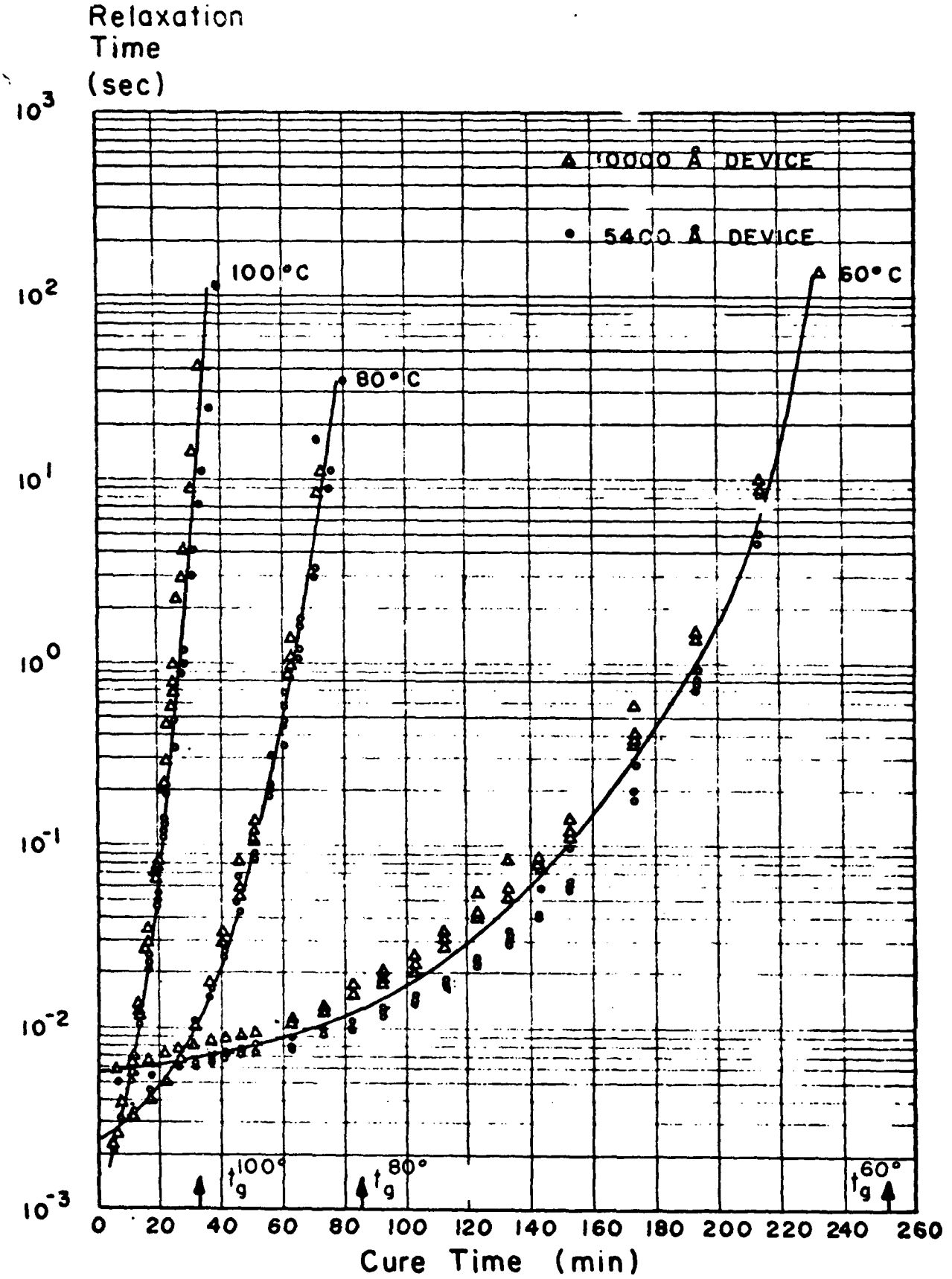
Relaxation
Time
(sec)
10^3
10^2
10^1
10^0
10^{-1}
10^{-2}
10^{-3}
▲ 10000 Å DEVICE
● 5400 Å DEVICE
100°C
80°C
60°C
$t_g^{100°}$
$t_g^{80°}$
$t_g^{60°}$
0 20 40 60 80 100 120 140 160 180 200 220 240 260
Cure Time (min)

FIG. 9

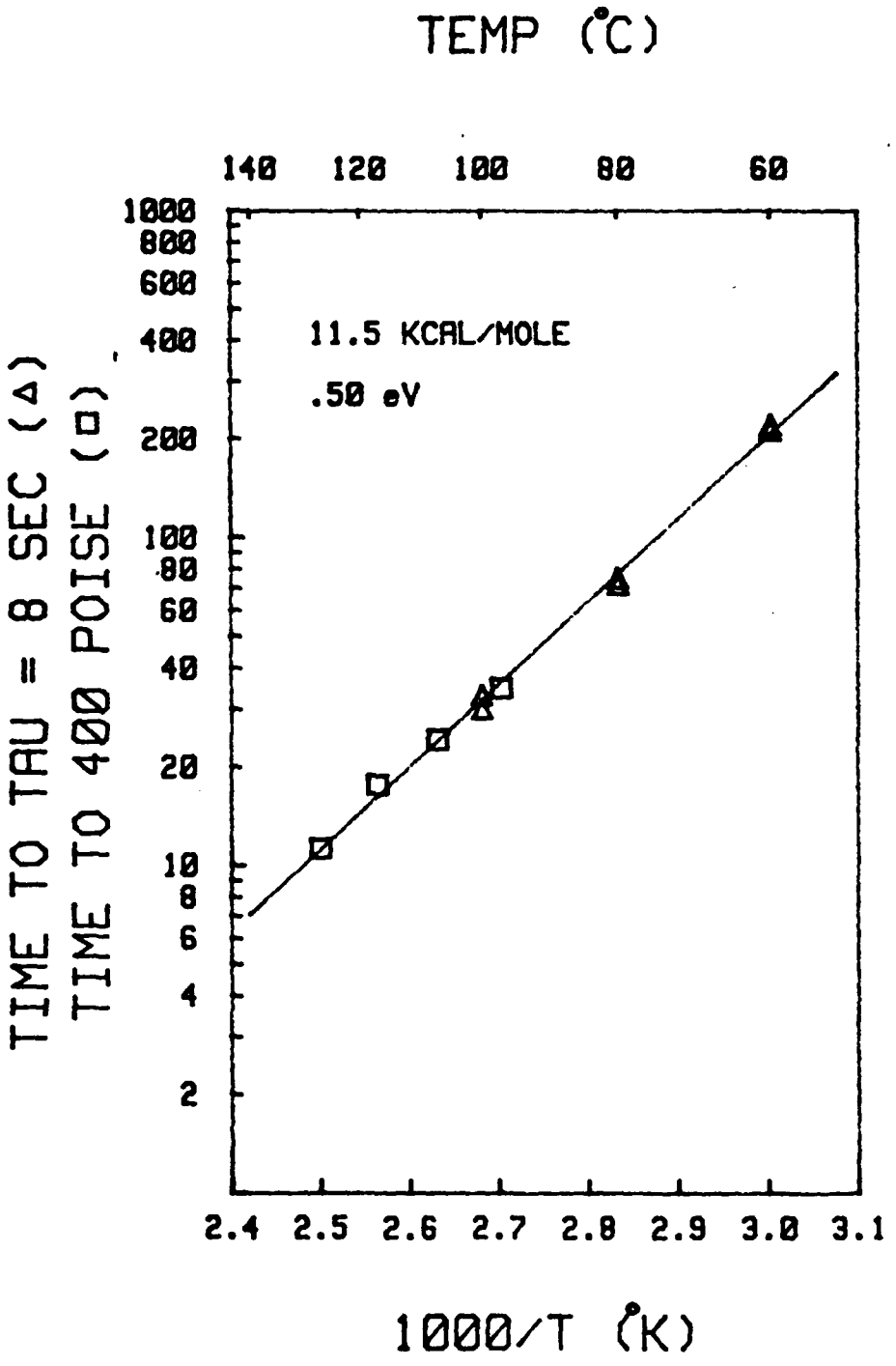
TEMP (°C)
140
120
100
80
60
1000
800
600
400
200
100
80
60
40
20
10
8
6
4
2
11.5 KCAL/MOLE
.50 eV
TIME TO TAU = 8 SEC (Δ)
TIME TO 400 POISE (□)
2.4
2.5
2.6
2.7
2.8
2.9
3.0
3.1
1000/T (°K)

FIG 10

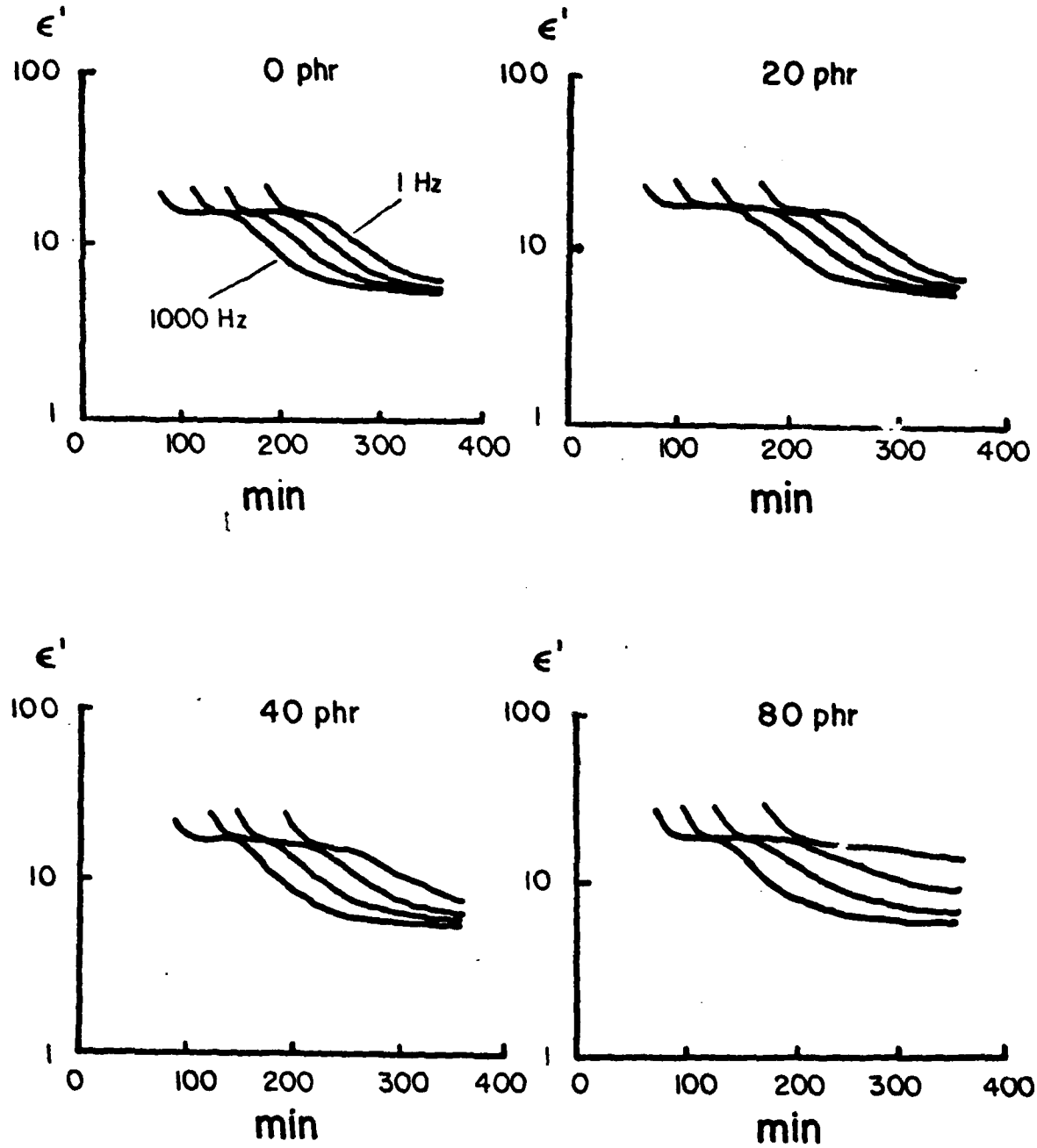
ε'
100
10
1
0 phr
1 Hz
1000 Hz
0
100
200
300
400
min
ε'
100
10
1
20 phr
0
100
200
300
400
min
ε'
100
10
1
40 phr
0
100
200
300
400
min
ε'
100
10
1
80 phr
0
100
200
300
400
min

FIG. 11

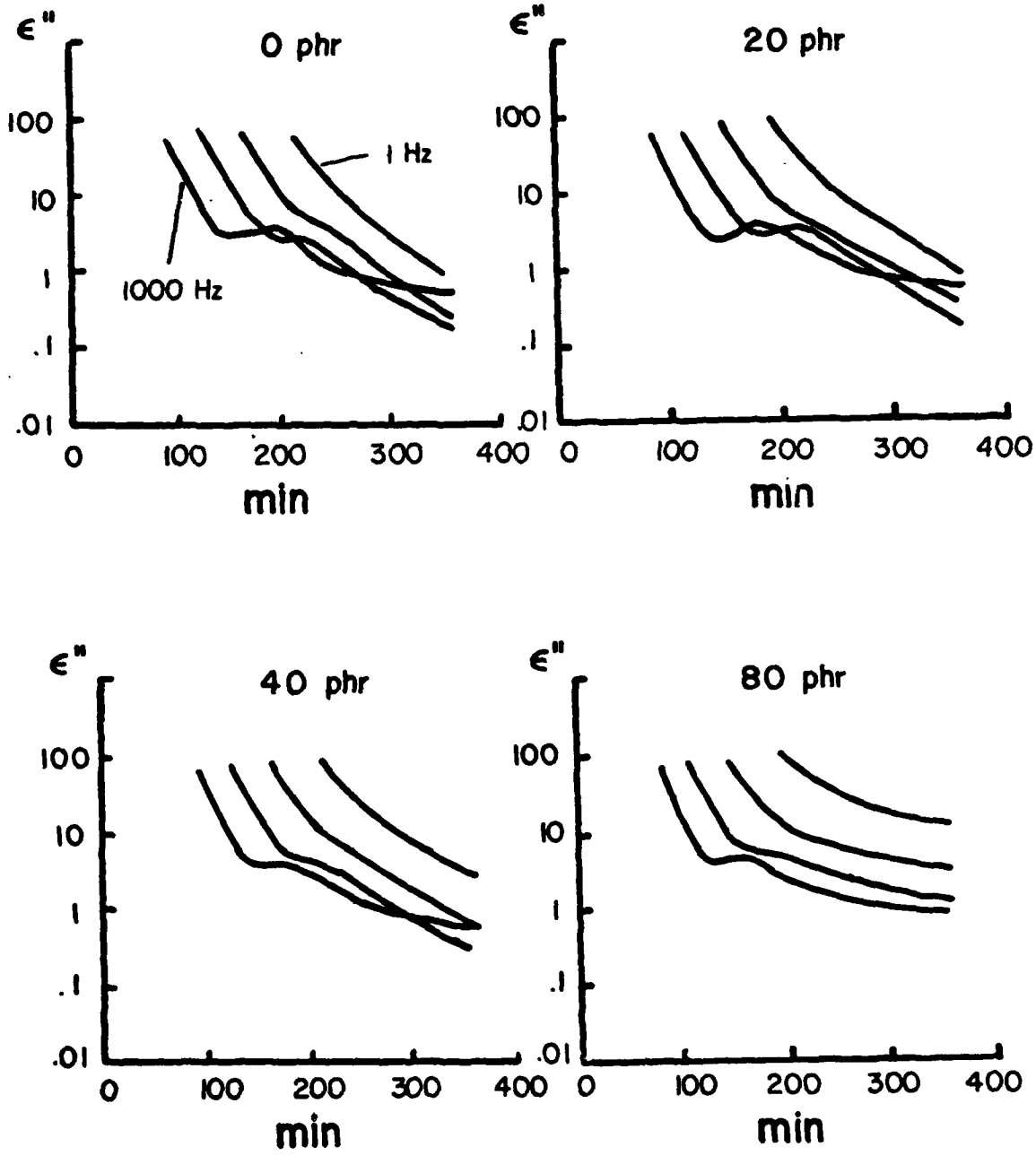
ε"
0 phr
100
10
1
.1
.01
1 Hz
1000 Hz
0
100
200
300
400
min
ε"
20 phr
100
10
1
.1
.01
0
100
200
300
400
min
ε"
40 phr
100
10
1
.1
.01
0
100
200
300
400
min
ε"
80 phr
100
10
1
.1
.01
0
100
200
300
400
min

FIG 12

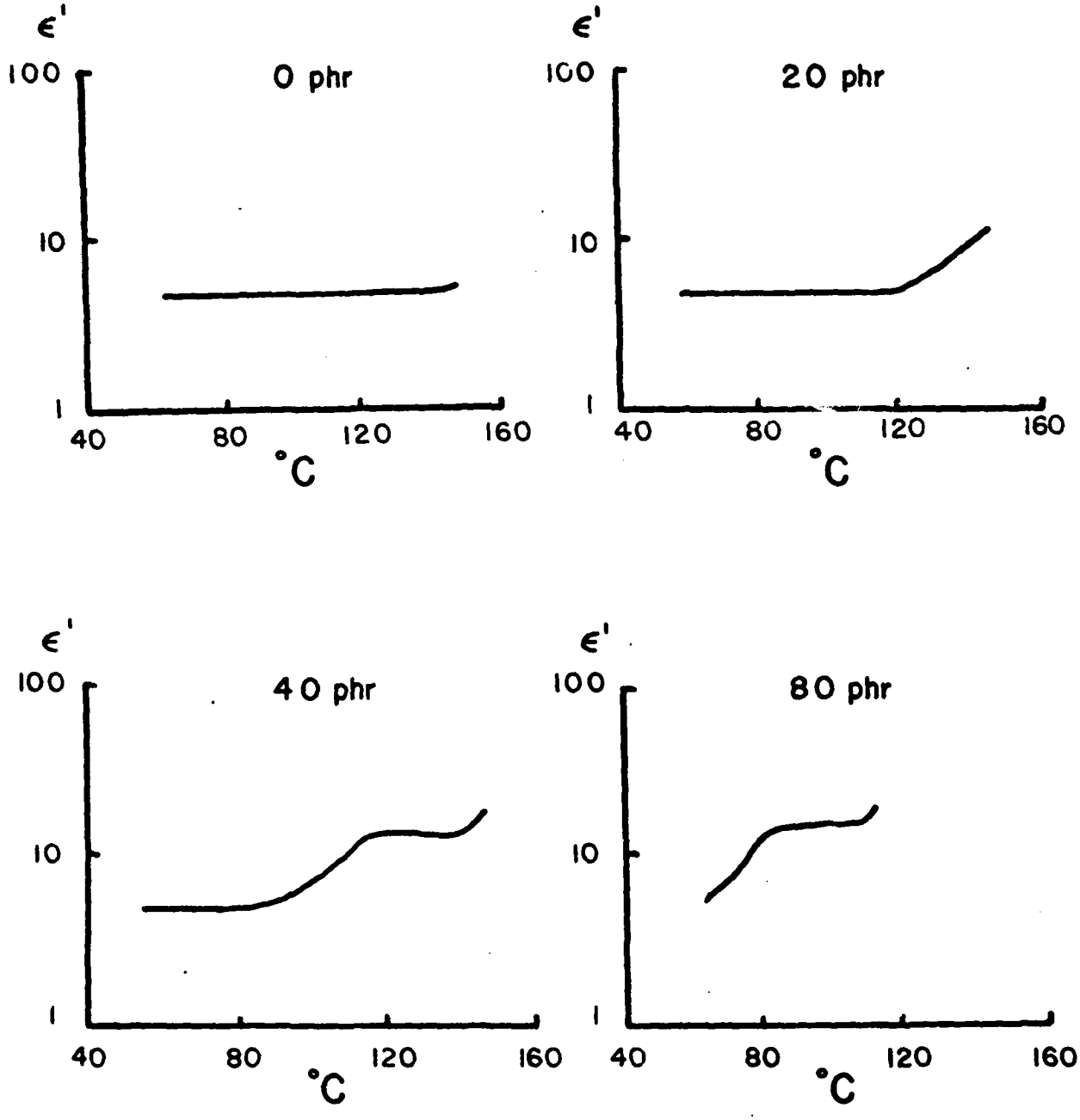
ε'
100
10
1
0 phr
40
80
120
160
°C
ε'
100
10
1
20 phr
40
80
120
160
°C
ε'
100
10
1
40 phr
40
80
120
160
°C
ε'
100
10
1
80 phr
40
80
120
160
°C

FIG 13

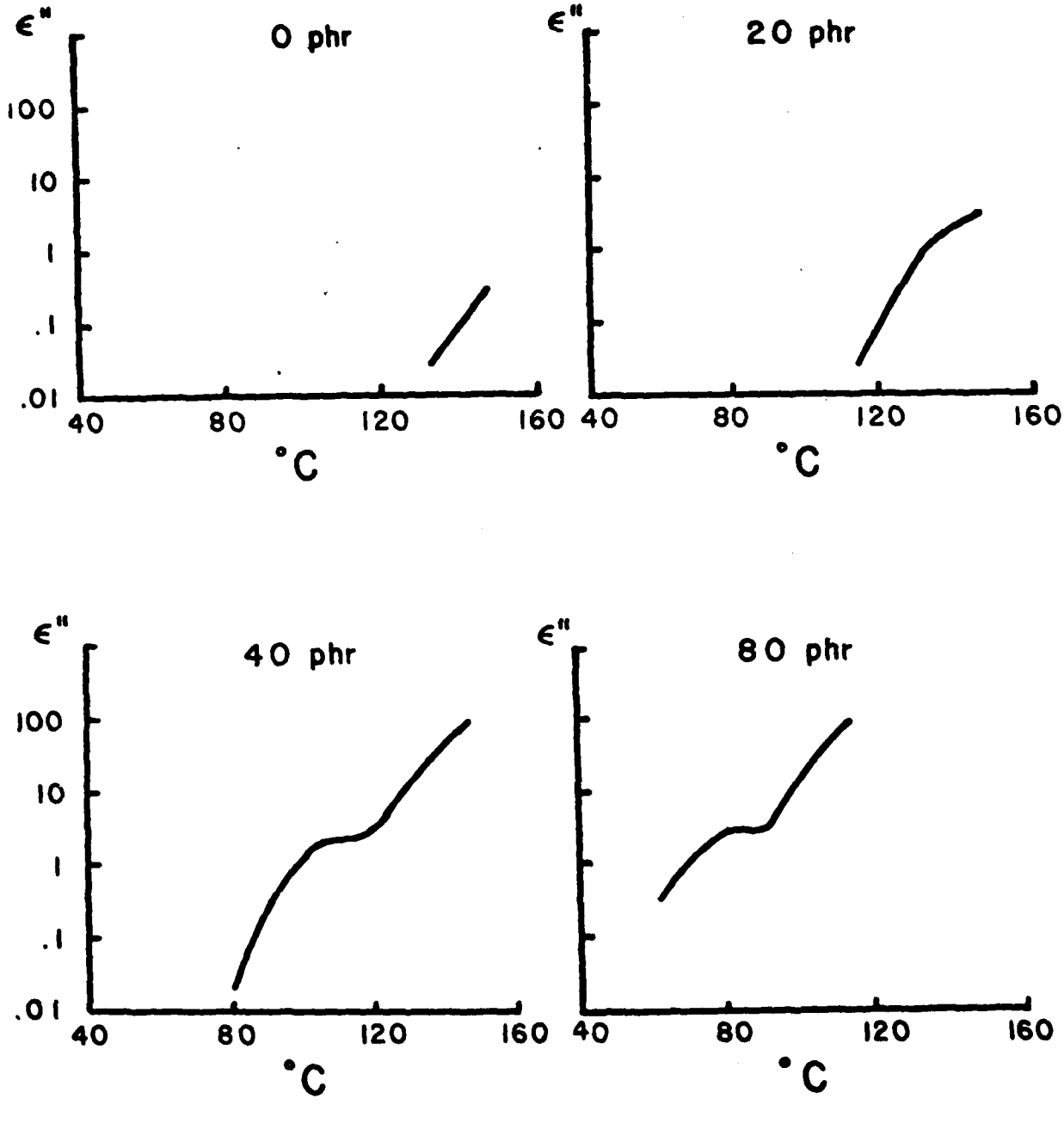
ε"
0 phr
100
10
1
.1
.01
40
80
120
160
°C
ε"
20 phr
40
80
120
160
°C
ε"
40 phr
100
10
1
.1
.01
40
80
120
160
°C
ε"
80 phr
40
80
120
160
°C

FIG. 14

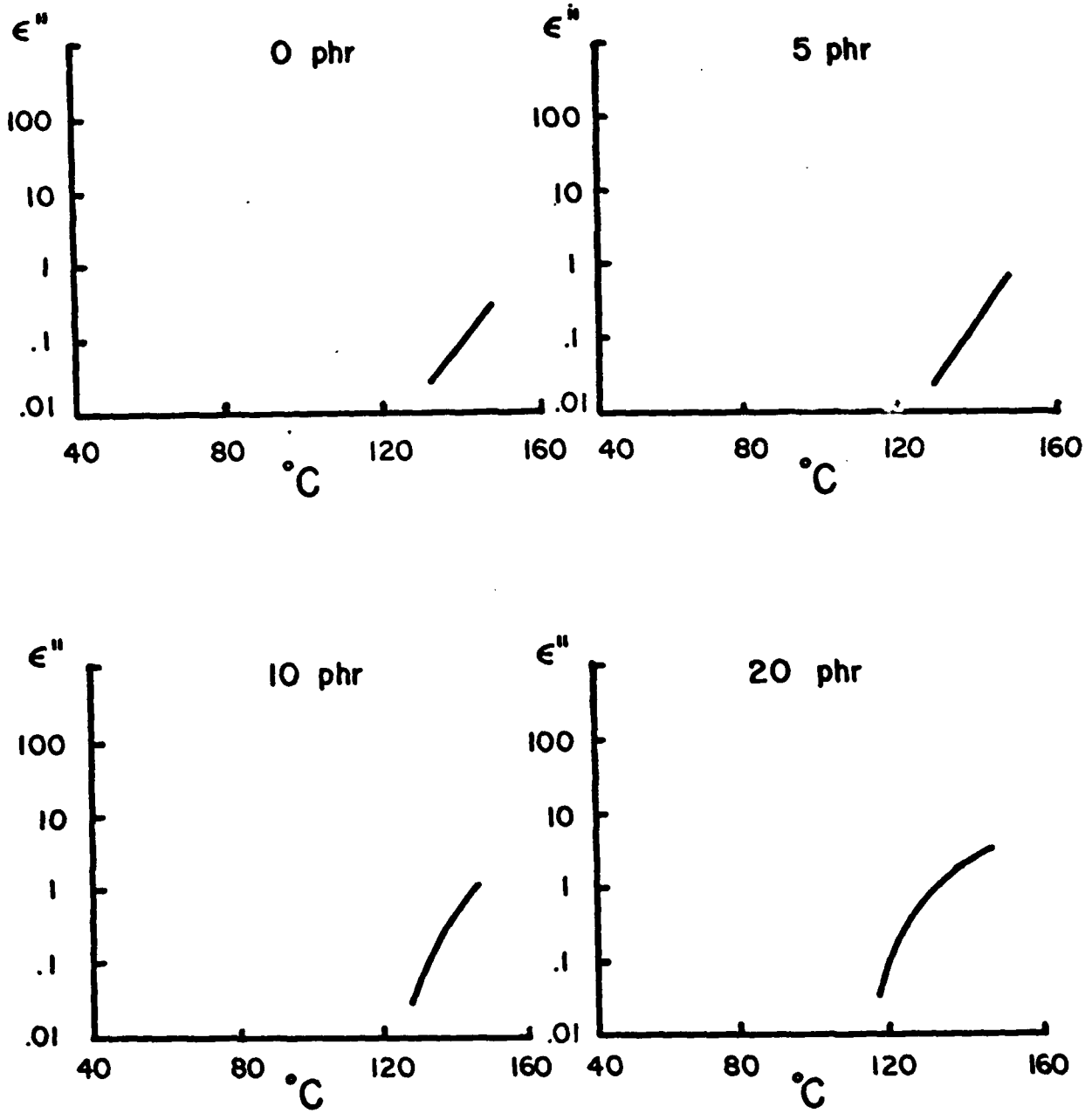
ε''
0 phr
100
10
1
.1
.01
40
80
120
160
°C
ε''
5 phr
100
10
1
.1
.01
40
80
120
160
°C
ε''
10 phr
100
10
1
.1
.01
40
80
120
160
°C
ε''
20 phr
100
10
1
.1
.01
40
80
120
160
°C

FIG 15

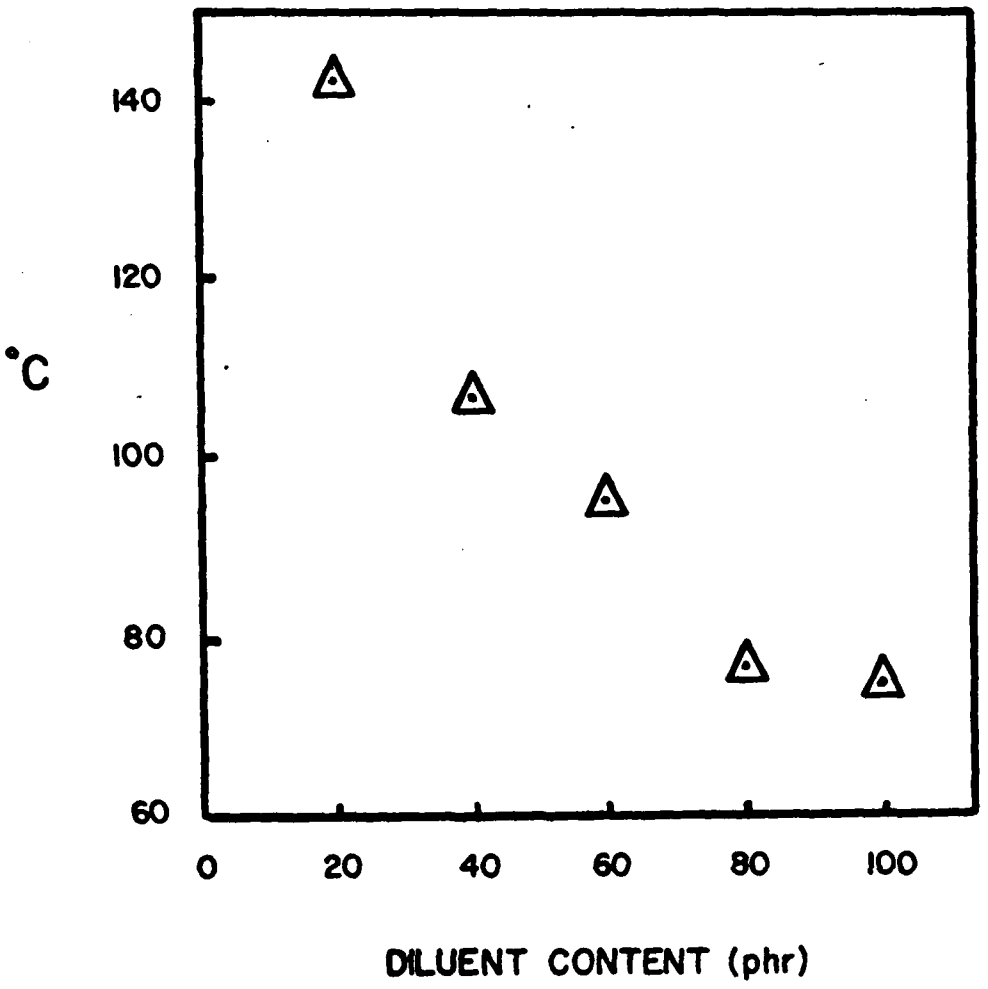

FIG 16

SP472-3/A1

472:GAN:716:ddc
78u472-608

TECHNICAL REPORT DISTRIBUTION LIST, GEN

	No. Copies
Office of Naval Research Attn: Code 472 800 North Quincy Street Arlington, CA 22217	(2)
ONR Branch Office Attn: Dr. George Sandoz 536 S. Clark Street Chicago, IL 60605	(1)
ONR Area Office Attn: Scientific Dept. 715 Broadway New York, NY 10003	(1)
ONR Western Regional Office 1030 East Green Street Pasadena, CA 91106	(1)
ONR Eastern/Central Regional Office Attn: Dr. L. H. Peebles Building 114, Section D 666 Summer Street Boston, MA 02210	(1)
Director, Naval Research Laboratory Attn: Code 6100 Washington, DC 20390	(1)
The Assistant Secretary of the Navy (RE S) Department of the Navy Room 4E736, Pentagon Washington, DC 20350	(1)
Commander, Naval Air Systems Command Attn: Code 310C (H. Rosenwasser) Department of the Navy Washington, DC 20360	(1)
Defense Technical Information Center Building 5, Cameron Station Alexandria, VA 22314	(12)
Dr. Fred Saalfeld Chemistry Division, Code 6100 Naval Research Laboratory Washington, DC 20375	(1)
U.S. Army Research Office Attn: CRD-AA-IP P. O. Box 1211 Research Triangle Park, NC 27709	(1)
Naval Ocean Systems Center Attn: Mr. Joe McCartney San Diego, CA 92152	(1)
Naval Weapons Center Attn: Dr. A. B. Amster, Chemistry Division China Lake, CA 93555	(1)
Naval Civil Engineering Laboratory Attn: Dr. R. W. Drisko Port Hueneme, CA 93401	(1)
Department of Physics Chemistry Naval Postgraduate School Monterey, CA 93940	(1)
Dr. A. L. Slafkosky Scientific Advisor Commandant of the Marine Corps (Code RD-1) Washington, DC 02380	(1)
Office of Naval Research Attn: Dr. Richard S. Miller 800 N. Quincy Street Arlington, VA 22217	(1)
Naval Ship Research and Development Center Attn: Dr. G. Bosmajian, Applied Annapolis, MD 21401	(1)
Naval Ocean Systems Center Attn: Dr. S. Yamamoto, Marine Sciences Division San Diego, CA 91232	(1)
Mr. John Boyle Materials Branch Naval Ship Engineering Center Philadelphia, PA 19112	(1)

Dr. Rudolph J. Marcus (1)
Office of Naval Research
Scientific Liaison Group
American Embassy
APO San Francisco 96503

Mr. James Kelley (1)
DTNSRDC Code 2803
Annapolis, MD 21402

Dr. Henry Wohltjen (1)
Code 6170
Office Of Naval Research
Arlington, VA 22217

Dr. Ron Trabocco (1)
Code 60631
Naval Air Development Center
Warminster, PA 18974

TECHNICAL REPORT DISTRIBUTION LIST

	No. Copies
Dr. Stephen H. Carr Department of Materials Science Northwestern University Evanston, IL 60201	(1)
Dr. M. Broadhurst Bulk Properties Section National Bureau of Standards U.S. Department of Commerce Washington, DC 20234	(2)
Prof. G. Whitesides Department of Chemistry Massachusetts Institute of Technology Cambridge, MA 02139	(1)
Prof. J. Wang Department of Chemistry University of Utah Salt Lake City, Utah 84112	(1)
Dr. V. Stannett Department of Chemical Engineering North Carolina State University Raleigh, NC 27607	(1)
Dr. D. R. Uhlmann Department of Metallurgy and Material Science Massachusetts Institute of Technology Cambridge, MA 02139	(1)
Naval Surface Weapons Center Attn: Dr. J. M. Augl, Dr. B. Hartman White Oak Silver Spring, MD 20910	(1)
Dr. G. Goodman Globe Union Incorporated 5757 North Green Bay Avenue Milwaukee, Wisconsin 53201	(1)
Picatinny Arsenal Attn: A. M. Anzalone, Bldg. 3401 SMUPA-FR-M-D Dover, NJ 07801	(1)
Dr. J. K. Gillham Department of Chemistry Princeton University Princeton, NJ 08540	(1)
Douglas Aircraft Co. Attn: Technical Library C1 290/36-84 AUTO-Sutton Long Beach, CA 90846	(1)
Dr. E. Baer Department of Macromolecular Science Case Western Reserve University Cleveland, OH 44106	(1)
Dr. K. D. Pae Department of Mechanics and Materials Science Rutgers University New Brunswick, NJ 08903	(1)
NASA-Lewis Research Center Attn: Dr. T. T. Serofini, MS-49-1 21000 Brookpark Road Cleveland, OH 44135	(1)
Dr. Charles H. Sherman Code TD 121 Naval Underwater Systems Center New London, CT 06320	(1)
Dr. William Risen Department of Chemistry Brown University Providence, RI 02192	(1)

Prof. Hatsuo Ishida (1)
Department of Macromolecular Science
Case-Western Reserve University
Cleveland, OH 44106

Mr. Robert W. Jones (1)
Advanced Projects Manager
Hughes Aircraft Company
Mail Station D 132
Culver City, CA 90230

Dr. C. Giori (1)
IIT Research Institute
10 West 35 Street
Chicago, IL 60616

Dr. M. Litt (1)
Department of Macromolecular Science
Case Western Reserve University
Cleveland, OH 44106

Dr. R. S. Roe (1)
Department of Materials Science
and Metallurgical Engineering
University of Cincinnati
Cincinnati, OH 45221

Dr. Robert E. Cohen (1)
Chemical Engineering Department
Massachusetts Institute of Technology
Cambridge, MA 02139

Dr. T. P. Conlon, Jr., Code 3622 (1)
Sandia laboratories
Sandia Corporation
Albuquerque, NM

Dr. Martin Kaufmann, Head (1)
Materials Research Branch, Code 4542
Naval Weapons Center
China Lake, CA 93555

Dr. Kurt Baum (1)
Fluorochem Inc.
6233 North Irwindale Avenue
Azuza, CA 91702
Cambridge, MA 02139

Dr. Alan Gent (1)
Department of Physics
University of Akron
Akron, OH 44304

Dr. T. J. Reinhart, Jr., Chief (1)
Composite and Fibrous Materials Branch
Nonmetallic Materials Division
Department of the Air Force
Air Force Materials Laboratory (AFSC)
Wright-Patterson AFB, OH 45433

Dr. J. Lando (1)
Department of Macromolecular Science
Case Western Reserve University
Cleveland, OH 44106

Dr. J. White (1)
Chemical and Metallurgical Engineering
University of Tennessee
Knoxville, TN 37916

Dr. J. A. Manson (1)
Materials Research Center
Lehigh University
Bethlehem, PA 18015

Dr. R. F. Helmreich (1)
Contract RD E
Dow Chemical Co.
Midland, MI 48640

Dr. R. S. Porter (1)
Department of Polymer Science
and Engineering
University of Massachusetts
Amherst, MA 01002

Prof. Garth Wilkes (1)
Department of Chemical Engineering
Virginia Polytechnic Institute and
State University
Blackburg, VA 24061

Prof. C. S. Paik Sung (1)
Department of Materials Science and
Engineering, Room 8-109
Massachusetts Institute of Technology